

**EXPERIMENTAL SEARCH FOR NARROW RESONANCES
IN THE REACTION $\pi^-p \rightarrow \gamma\gamma n$ AT 13 GeV/c^{*}**

I.H. CHIANG, R.A. JOHNSON, B.P. KWAN, T.F. KYCIA, K.K. LI,
L.S. LITTENBERG, A.R. WIJANGCO¹

Brookhaven National Laboratory, Upton, NY 11973, USA

A.M. HALLING², G.E. HOGAN³, C.G. LU⁴, K.T. McDONALD, A.J.S. SMITH, M.H. YE⁴

Princeton University, Princeton, NJ 08544, USA

and

L.A. GARREN⁵ and J.J. THALER

University of Illinois, Urbana, IL 61801, USA

Received 28 February 1984

Using a double arm electromagnetic calorimeter we have searched for narrow states produced in the exclusive reaction $\pi^-p \rightarrow \gamma\gamma n$ at 13 GeV/c. No enhancements were observed in the mass range 2.0–4.0 GeV/c². For example, the 90% confidence limit on η_c production is $\sigma(\pi^-p \rightarrow \eta_c n) \times B(\eta_c \rightarrow \gamma\gamma) < 44$ pb.

Although there now exists a coherent picture of charmed quark spectroscopy and of e^+e^- annihilations into charmed particles, the *hadronic* production of new narrow states is still not well understood, either experimentally or theoretically. For example, although comprehensive data have been compiled for J/ψ production by hadrons, the 1S_0 charmonium states η_c and η'_c still have not even been observed in hadronic collisions. In the most sensitive search so far for narrow states with even charge conjugation, a Serpukhov ex-

periment observed [1] a narrow state $X^0(2.8 \text{ GeV}/c^2)$, in the reaction $\pi^-p \rightarrow \gamma\gamma n$ at 40 GeV/c. Developments [2,3] since that work indicate that the X^0 is not the η_c , reopening the question of the nature of the object. In addition, it has been suggested [4] that four-quark bound states may exist in the 2–4 GeV mass region. In an attempt to confirm the X^0 and to search for the hadronic production of the η_c , η'_c and other narrow two-photon states we have performed an experiment to measure the exclusive reaction $\pi^-p \rightarrow X^0 n$; $X^0 \rightarrow \gamma\gamma$ at 13 GeV/c.

The apparatus is indicated schematically in fig. 1a. A 13 GeV/c π^- beam produced at the Brookhaven AGS interacted in a scintillator target 3.13 cm in diameter and 30.5 cm long. The target was divided longitudinally into 6 segments. As the final state consists entirely of neutral particles it was possible to localize the interaction vertex within ± 1 cm. The neutron was not detected. The photons were detected by two large 107 cm \times 213 cm calorimeters located 560 cm downstream of the target at $\pm 16.4^\circ$ with respect to the π^-

^{*} This experiment, performed at Brookhaven National Laboratory, was supported by the US Department of Energy.

¹ Permanent address: Actagen Corp., Elmsford, NY 10523, USA.

² Permanent address: Cornell University, Ithaca, NY 14853, USA.

³ Permanent address: Temple University, Philadelphia, PA 19122, USA.

⁴ Permanent address: Institute of High Energy Physics, Beijing, China.

⁵ Permanent address: Vanderbilt University, Nashville, TN 37235, USA.

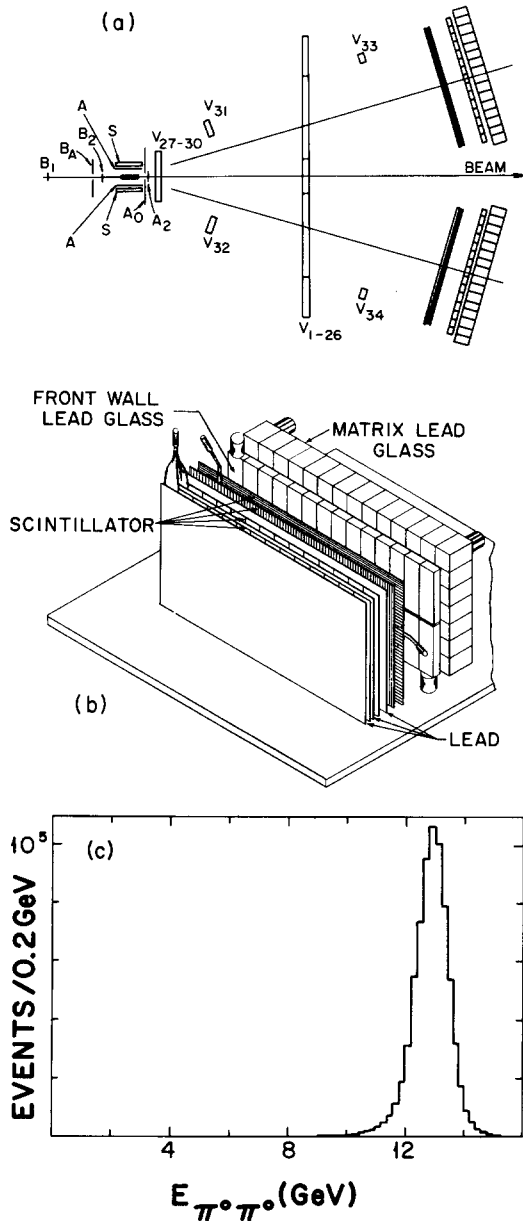


Fig. 1. (a) Plan view of detector. (b) Expanded view of photon calorimeter. (c) Energy distribution of $\pi^0\pi^0$ in detected $\pi^-p \rightarrow \pi^0\pi^0n$ events.

beam line. One of these calorimeters is shown in fig. 1b. First came a converter section consisting of 3 layers of lead, each 1.3 radiation lengths (r.l.) thick. The first 2 layers were each followed by a plane of 15

cm wide scintillator strips. The third layer of lead was followed by two planes of 2.5 cm wide "finger" scintillation counters, which located shower vertices to ± 6 mm vertically and horizontally, and augmented the calorimetry measurement. Following the converter section were two walls of lead-glass blocks. The front 15×2 array consisted of blocks 15 cm wide \times 45 cm high \times 3 r.l. deep; the rear 16×7 matrix was composed of blocks 15 cm \times 15 cm \times 9 r.l. deep.

Surrounding the target on 4 sides were scintillation veto counters A, which were used with vetoes A0 and A2 downstream to identify an all-neutral final state. Photons not within the calorimeter aperture were vetoed by sets of lead-scintillator shower counters S (just outside the A counters) and V (distributed downstream). An interaction triggered the readout system if the following requirements were satisfied: (1) a neutral final state, (2) no hits in S or V, (3) at least 1 GeV energy in each calorimeter arm, and (4) more than 9 GeV in both calorimeter arms combined. For each trigger, pulse-height and time-of-flight information were recorded for each of the 648 detector elements. During normal running the beam intensity was $10^7 \pi^-$ per 1 second burst, so timing information was essential to reject signals from out-of-time interactions. An absolute calibration of the detectors was obtained in place by diverting 6 GeV electrons into each element of the calorimeters. Relative calibration was accomplished on the long term by measuring the pulse height from small radioactively-doped scintillators glued to each counter, and on the short term from light fanned out from a spark gap by fiber optics. The fractional energy resolution achieved for electrons was $\sigma_E/E = 0.14/\sqrt{E}$ (E in GeV).

The acceptance of the detector at 13 GeV/c lies in the mass range 1.8–4.0 GeV/c², in which there are no prominent resonances to use for calibration. Therefore, we also took data at π^- momenta of 8.5 and 5.0 GeV/c to measure the reactions $\pi^-p \rightarrow (\eta, \eta', \omega) + n$. As a further test the beam and target were aligned with the center of one spectrometer arm to measure $\pi^-p \rightarrow (\pi^0, \eta)n$. The results of π^0 , η , η' , and ω production were in adequate agreement with previous data, giving us confidence in our calculations of acceptance and mass resolution. Information from these runs was used along with the electron beam data described above to determine the calibration constants for the different layers of the calorimeter.

During the experiment approximately 5×10^6 events satisfying the normal trigger requirements were recorded. The vast majority were $\pi^- p \rightarrow \pi^0 \pi^0 n$ events in which all 4 γ 's hit the active area of the detector, or in which one soft γ struck a veto counter but deposited less than the threshold energy of 60 MeV. The events were processed by a pattern recognition program which combined contiguous pulse height depositions into clusters and then classified the clusters as one- or two-photon showers. We found that a photon had a $\sim 95\%$ probability of making an identifiable shower in the finger counters, and that the shower energy was confined to 2 or 3 counters. Since the minimum separation between the two γ 's from a maximum energy π^0 was ~ 6 finger counters, 90% of the π^0 's in which both γ 's struck the calorimeters were immediately recognized. If only one γ shower appeared in the finger counters, the other γ converting in the lead-glass, the π^0 was recognized with 98% efficiency either by the failure of the shower in the finger counter ($\sigma_{x,y} \sim 6$ mm) to line up with the shower in the lead-glass ($\sigma_{x,y} \sim 12$ mm) or by the recognition of two showers in the lead-glass matrix. Therefore only 0.2% of π^0 's in which both γ 's struck the detector were mistaken for single γ 's. As discussed below, a more serious source of apparent single γ 's was from very asymmetric π^0 decays in which the low-energy γ escaped detection by falling below the 60 MeV veto threshold.

Fig. 1c shows the measured energy spectrum for $\pi^- p \rightarrow \pi^0 \pi^0 n$ events. The clean peak near 13 GeV is evidence of the effectiveness of trigger and event-selection procedures. Kinematic fitting, using the (missing) mass of the neutron as a constraint, reduced the estimated error in the $\gamma\gamma$, $\pi^0\gamma$, and $\pi^0\pi^0$ effective masses $^{\pm 1}$ to ~ 48 MeV/ c^2 at 2.8 GeV/ c^2 . Fig. 2a shows, as a function of mass, the numbers $N(M)$ of $\pi\pi$, $\pi\gamma$, and $\gamma\gamma$ events detected, uncorrected for acceptance. No significant narrow enhancements are evident. Monte Carlo studies show that the $\pi^0\gamma$ and $\gamma\gamma$ samples are, in fact, consistent with the background from $\pi^0\pi^0$ events in which one γ or two γ 's, respectively, escaped detection. This "feed-down" hypothesis predicts that the $\gamma\gamma$ background $N_{\gamma\gamma}(M)$ is related to $N_{\pi\gamma}(M)$ and $N_{\pi\pi}(M)$ as follows:

^{±1} The resolution in effective mass varied from 30 MeV/ c^2 at 1.8 GeV/ c^2 to 68 MeV/ c^2 at 3.8 GeV/ c^2 .

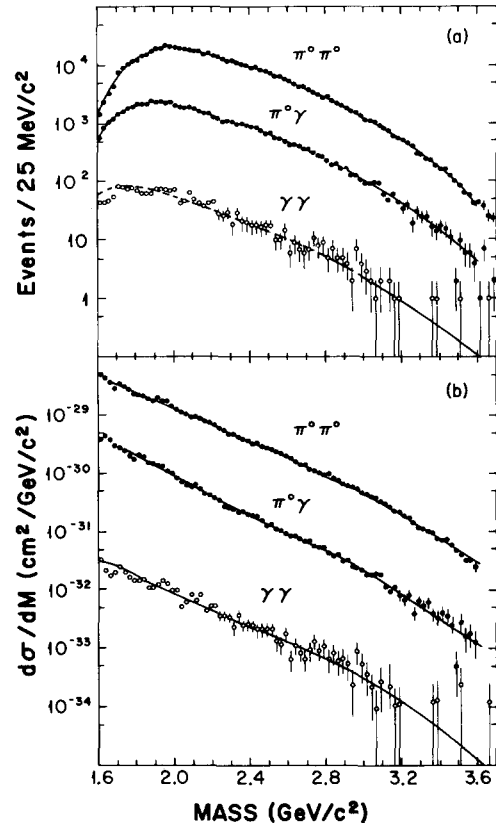


Fig. 2. Mass distributions of $\pi^0\pi^0$, $\pi^0\gamma$ and $\gamma\gamma$ events. The curves were obtained as described in the text. (a) Event distributions, uncorrected for acceptance. (b) Total cross sections as a function of mass, extrapolating to the entire regions of t and $\cos\theta$ from the measured regions using the assumptions described in the text.

$$N_{\gamma\gamma}(M) = N_{\pi\pi}(M) \times \{N_{\pi\gamma}(M) / [2N_{\pi\pi}(M)]\}^2. \quad (1)$$

The curves in fig. 2a for the $\pi\pi$ and $\pi\gamma$ spectra are 6th order polynomial fits to the logarithms of $N_{\pi\pi}(M)$ and $N_{\pi\gamma}(M)$. Substituting these expressions into eq. (1) gives the *predicted* curve for $N_{\gamma\gamma}(M)$ also shown in fig. 2a. The agreement both in shape and absolute normalization with the observed $\gamma\gamma$ spectrum is striking. The χ^2 is 59 for 60 degrees of freedom, indicating that all $\gamma\gamma$ events can be accounted for by feed-down from the dominant $\pi^0\pi^0$ process.

The spectra have been corrected for acceptance to give the absolute cross sections shown in fig. 2b. Corrections were also made for shower recognition efficiency, beam attenuation in the target, and losses

from goodness of fit cuts. The event sample is limited to the momentum transfer region $|t_{\min}| < |t| < (|t_{\min}| + 0.4 \text{ GeV}/c^2)$, and to the region of decay angle $|\cos \theta| < 0.4$ with respect to the beam direction, measured in the rest frame of the decaying neutral state. Hence, knowledge of the production mechanism of the pairs is needed to make an absolute normalization. The $\pi^0\pi^0$ data are consistent with the form $d\sigma/dt \sim e^{6t}$ over the above limited range; the angular distribution is roughly isotropic. The cross sections given in fig. 2b are extrapolated over the entire t and $\cos \theta$ region using the above form. The $\pi^0\pi^0$ mass spectrum falls roughly as $d\sigma/dM \sim e^{-3.4M}$. The probability of a π^0 appearing to be a single γ was 2.5%.

To set limits on the production of narrow resonances decaying to $\gamma\gamma$, we have fitted the $\gamma\gamma$ data in the mass range 2.0–3.2 GeV/c^2 to a combination of the feed-down spectrum described above and a single gaussian, whose width was taken to be the detector resolution. Each 25 MeV/c^2 region was tested in turn, by constraining the center of the resonance to lie within it. The result is shown in fig. 3, where the $\gamma\gamma$ event distribution, uncorrected for acceptance, is shown (data points) with the feed-down from $\pi^0\pi^0$ subtracted. Effects of marginal significance were found 2.0 GeV/c^2 (2σ), 2.15 GeV/c^2 (2.5σ), 2.78 GeV/c^2 (1.5σ), and 2.95 GeV/c^2 (0.7σ). Since there are no compelling candidates, we have used this distribution to obtain the 90% upper limits shown as the solid curve in fig. 3. The limit on $\sigma(\pi^-p \rightarrow \eta_c n) \cdot B(\eta_c \rightarrow \gamma\gamma)$ is 44 pb, with 90% confidence. Although this is the most sensitive search yet for η_c production in hadronic collisions, it does not reach the few-pb level of recent theoretical estimates [5]. On the other hand, it rules out models in which there are large threshold enhancements [6], or large mixing between light and charmed quarks [7]. It is interesting to note that a fluctuation appears in the same region as the X^0 reported in ref. [1]. To compare the two results it is necessary to take into account the difference in beam energy between the two experiments. The process $\pi^-p \rightarrow \eta_c n$ is expected to proceed mainly via A_2 exchange, as do $\pi^-p \rightarrow \eta n$ and $\pi^-p \rightarrow \eta' n$. The cross section would be expected [8] to scale as $p^{-\alpha} f(t_{\min})$, where $1 < \alpha < 1.5$, and where $f(t_{\min})$ is 1.8 times larger at 40 GeV/c than at 13 GeV/c . Then

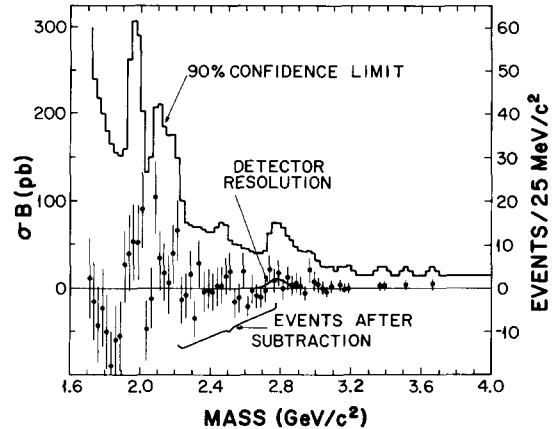


Fig. 3. The data points show the number of $\gamma\gamma$ events per 25 MeV/c^2 interval, after the predicted number of feed-down events from eq. (1) have been subtracted. These data are uncorrected for apparatus acceptance. The solid curve gives the 90% upper limits, as a function of mass, on σ_B for narrow resonances decaying to $\gamma\gamma$.

the 200 pb cross section at 40 GeV/c reported in ref. [2] would imply a cross section of 330–550 pb at 13 GeV/c , in clear disagreement ^{#2} with our upper limit of 78 pb. Any object other than a pseudoscalar, such as a four-quark object hypothesized by Lipkin et al. [4], would be expected to have a much more steeply falling p dependence, making the work of ref. [1] in even worse disagreement with our result.

^{#2} In ref. [2], the cross section is measured for $|t| > 0.15 \text{ GeV}/c^2$; our experiment covers a very similar region $|t| > |t_{\min}| = 0.14 \text{ GeV}/c^2$.

References

- [1] W.D. Apel et al., Phys. Lett. 72B (1978) 500.
- [2] R. Partridge et al., Phys. Rev. Lett. 44 (1980) 712.
- [3] A.Yu. Khodjamirian, Phys. Lett. 90B (1980) 460.
- [4] H.J. Lipkin et al., Phys. Lett. 78B (1978) 295.
- [5] C. Quigg and R.D. Field, Fermilab Report 75/15 THY (1975);
H. Fritzsch and J.D. Jackson, Phys. Lett. 66B (1977) 365.
- [6] E.L. Berger and C. Sorenson, Phys. Lett. 62B (1976) 303.
- [7] H. Harari, Phys. Lett. 60B (1976) 172.
- [8] G. Eilam et al., Phys. Lett. 80B (1979) 306.